Atmospheric HCFC-22, HFC-125 and HFC-152a at Cape Point, South Africa

Brett Kuyper[1], Daniel Say[2], Casper Labuschagne[3], Timothy Lesch[1], Warren R. Joubert[3], Damien Martin[2], Dickon Young[2], M. Anwar H. Khan[2], Matthew Rigby[2], Anita L. Ganesan[4], Mark F. Lunt[5], Colin O'Dowd[6], Alistair J. Manning[2,7], Simon O'Doherty[2], Michael T. Davies-Coleman[1], Dudley E. Shallcross[1,2]

[1]Department of Chemistry, University of the Western Cape, Bellville 7535, South Africa

[2]Atmospheric Chemistry Research Group, School of Chemistry, University of Bristol, Bristol, BS8 1TS, United Kingdom

[3]Climate and Environmental Research and Monitoring, South African Weather Service, Stellenbosch 7600, South Africa

[4]School of Geographical Sciences, University of Bristol, Bristol, BS8 1SS, United Kingdom

[5]School of Geosciences, University of Edinburgh, Edinburgh, EH9 3JW, United Kingdom

[6]School of Physics, Ryan Institute's Centre for Climate and & Pollution Studies, and Marine Renewable Energy Ireland, National University of Ireland Galway, Galway. H91 CF50, Ireland

[7]Hadley Centre, The Met Office, Exeter, EX1 3PB, United Kingdom

ABSTRACT

One hydrochlorofluorocarbon and two hydrofluorocarbons (HCFC-22, HFC-125 and HFC-152a) were measured in air samples at the Cape Point observatory (CPT), South Africa during 2017. These data represent the first such atmospheric measurements of these compounds from south western South Africa (SWSA). Baseline atmospheric growth rates were estimated to be 8.36 ppt yr^{-1}, 4.10 ppt yr^{-1} and 0.71 ppt yr^{-1} for HCFC-22, HFC-125 and HFC-152a, respectively. The CPT measurements were combined with an inverse model to investigate emissions from SWSA. For all three halocarbons, Cape Town was found to be the dominant source within SWSA. These estimates were extrapolated, based on population statistics, to estimate emissions for the whole of South Africa. We estimate South Africa's 2017 emissions to be 3.0 (1.6 – 4.4) Gg yr^{-1}, 0.8 (0.5 – 1.2) Gg yr^{-1} and 1.1 (0.6 – 1.6) Gg yr^{-1} for HCFC-22, HFC-125 and HFC-152a, respectively. For all three halocarbons, South Africa's contribution to global emissions is small (<2.5%), but future monitoring is needed to ensure South Africa's compliance with regulation set out by the Montreal Protocol and its Amendments.

Keywords: HFCs; HCFCs; South Africa; climate; greenhouse gases; ozone depleting substances; emissions

INTRODUCTION

The phasing-out of the industrial production of chlorofluorocarbons (CFCs), as a direct consequence of the Montreal Protocol, has led to an increase in the production and use of hydrochlorofluorocarbons (HCFCs) and hydrofluorocarbons (HFCs) as substitutes, commonly used as refrigerants in air conditioners and in the production of insulating foams. HCFCs and HFCs also find widespread applications as solvents used in lubricants, coatings and cleaning fluids. The presence of a reactive hydrogen atom in the molecular structures of HCFCs and

HFCs results in these compounds being more susceptible to attack and degradation in the troposphere through reaction with hydroxyl radicals (OH).[1,2] HFCs have zero Ozone Depletion Potentials (ODP) as they contain no chlorine or bromine atoms and, despite the presence of chlorine in HCFCs these compounds have lower ODPs than the CFCs they replace.[3] Conversely, HCFCs and HFCs both have an immediate and significant effect on the Earth's climate due to their high global warming potentials (GWP).[4,5] Given their non-negligible ODPs and high GWPs,[6] the industrial production of HCFCs has been controlled under the Montreal Protocol and its amendments since 1992, and owing to their high GWPs, the production of HFCs will now be regulated following the Kigali amendment to the Protocol.[7,8] Specifically, the HCFC Phase-out Management Plan (HPMP) seeks to define targets for the reduction of HCFC consumption in developing countries such as South Africa. Under stage two of the HPMP, these countries agreed to freeze their consumption of HCFCs by 2013, followed by a 10% reduction by 2016. A complete ban on the production and consumption of HCFCs for dispersive (emitted to the atmosphere) applications is planned for 2030.[9] South Africa is also expected to ratify the Kigali Amendment to the Montreal Protocol, which sets out phase-down targets for HFCs. However, the majority of developing countries will not be required to freeze production/consumption of HFCs until 2024.

HCFC-22 ($CHClF_2$), which has a tropospheric lifetime of 11.9 years,[10] was introduced in the early 1990s as a replacement for CFCs and is the most abundant HCFC in the atmosphere.[11] The GWP of HCFC-22 is 1760 integrated over a 100-yr time horizon (GWP_{100}),[10] and its ODP is 0.055.[12] The principal removal process for this compound from the atmosphere is reaction with OH ($k_{OH} = 5.0 \times 10^{-15}$ cm^3 $molecule^{-1}$ s^{-1} at 298 K).[13] Following a maximum global mean growth rate in 2007 of 8.2 ppt yr^{-1}, the rate of growth had decreased by 2015 to 3.7 ppt yr^{-1} (-54%).[12]

Global emissions of HCFC-22 have now stabilized at approximately 370 Gg yr^{-1} (2016) due to the freezing of HCFC production and consumption for dispersive uses in developing countries.[10,14] Production is limited to existing chemical plants and no increase in production is permitted under the Montreal Protocol guidelines. Currently, the main source of emission of HCFC-22 into the atmosphere is a result of leakage from refrigeration equipment either during use, servicing or final disposal, rather than from the chemical plants in which it is produced.[15] Traditionally, emissions from leakage and servicing were thought to be relatively constant throughout the year.[16] However, more recent studies have suggested that there is significant seasonality in the emission rates of HCFC-22. Xiang et al.[17] estimated that emissions of HCFC-22 were over twice as large during summer months, compared with winter months. While this seasonal cycle is observed globally, the magnitude is larger in the northern hemisphere.[17] The authors proposed that the increased usage rates and ambient temperatures (resulting in greater charge pressures and hence greater leakage) generally associated with summer months as potential reasons for the observed seasonality.

HFC-125 (CF_3CHF_2) is the third most abundant HFC (after HFC-134a and HFC-23) and currently makes the third largest contribution of the HFCs to atmospheric radiative forcing with a GWP_{100} of 3500.[10,18,19] The atmospheric lifetime of HFC-125 is estimated to be 31 years,[10] and this trace gas is removed from the atmosphere by reaction with OH resulting in *inter alia* carbonyl fluoride and trifluoromethanol degradation products. In 2015, the global average mole fraction of HFC-125 was 18.4 ppt in the lower troposphere with an estimated growth of 2.3% per annum for the period of 1995-2015.[12] HFC-125 is almost exclusively used in blends with HFC-134a, HFC-143a and HFC-32. Common examples of these blends include R-410A (50% by wt. HFC-125, 50% by wt. HFC-32) and R-407C (52% by wt. HFC-134a, 25% by wt. HFC-125, 23%

by wt. HFC-32). Due to widespread application as an HCFC-22 replacement in commercial refrigeration, which as a group experiences loss rates of around 30% per year, HFC-125 mole fractions have been rapidly rising.[22-24]

HFC-152a (CH_3CHF_2) has a relatively small GWP_{100} of 138,[18] and a significantly shorter atmospheric lifetime of approximately 1.5 years,[10,20] compared with other HFCs. Consequently, HFC-152a is often used as a replacement for CFCs, various HCFCs and HFC-134a in technical aerosol applications, foam blowing and mobile air-conditioners. A rapid accumulation of HFC-152a in the atmosphere up to 2012, with increases of 8.9 ppt (1992 – 2012) and 3.7 ppt (1998 – 2012) for the Northern and Southern Hemispheres respectively, were reported.[20] However, the global mean mole fraction has since stabilized, with a global mean growth rate post-2012 that does not differ significantly from 0 ppt yr^{-1} (-0.06 ± 0.05 ppt yr^{-1}).[20] Global emissions were estimated to be 52.5 ± 20.1 Gg yr^{-1} in 2014.[20]

Given the greater population and industrialization in the Northern Hemisphere, a North-South interhemispheric gradient has been established for all of these compounds.[12,20] The number of *in-situ* measurements of HCFCs and HFCs available from Northern Hemispheric sites exceeds those available from the Southern Hemisphere. Continuous measurements of three CFCs (CFC-11, CFC-12 and CFC-113) and TCE have been made at the Cape Point Global Atmospheric Watch Station, South Africa over the period 1979-2015.[21] Extension of the range of tropospheric HCFC and HFC concentrations measured at sites in the Southern Hemisphere is required for more robust constraints on global, southern-hemispheric and regional emissions estimates. In this study, we report the 2017 time series of atmospheric mole fractions of HCFC-22, HFC-125 and HFC-152a at Cape Point, South Africa. We consider variations in the mole fractions of each compound with respect to various meteorological parameters (e.g. wind speed and direction) and use an inverse model to provide the first documented top down emissions estimates of HCFC-22, HFC-125 and HFC-152a for South Africa.

METHODS

Global Atmospheric Watch Monitoring station

The South African Weather Service manage and maintain the Global Atmospheric Watch (GAW) monitoring station at Cape Point (34.5º S, 18.2º E)[21] situated approximately 60 km south of the City of Cape Town (population ~4 million). The station is situated on an elevated peninsula (230 m above sea level) extending out into the south Atlantic (Figure 1). The local seasonal synoptic patterns around Cape Town results in predominantly clean marine air arriving at Cape Point during austral summer and occasionally anthropogenically modified air arriving during austral winter.[21,22] The differing air mass sources are driven by the South Atlantic High Pressure (SAHP) system which occupies a latitudinal position roughly in line with Cape Town during summer, driving strong south-easterly winds, drawing air from deep in the south Atlantic, towards Cape Point.[22–24] The SAHP system retreats to the north during austral winter, thus allowing transient low-pressure systems to impact Cape Town and Cape Point.[22–25]

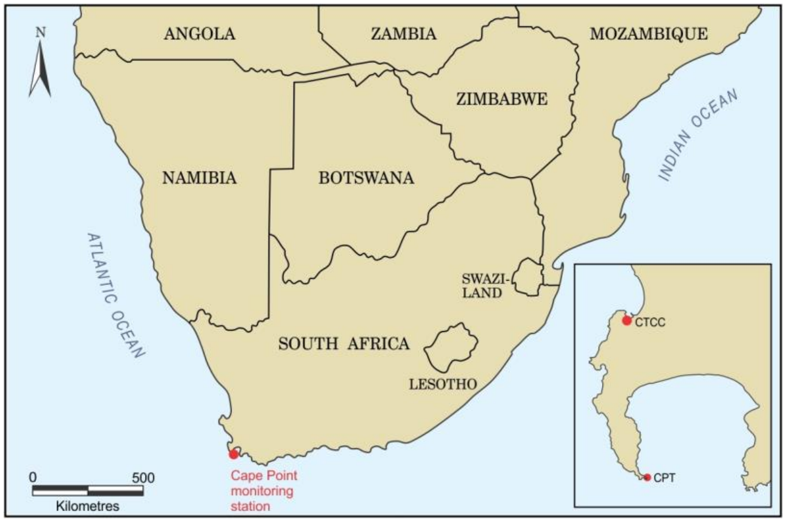

Figure 1. GAW monitoring station at Cape Point in relation to the south Atlantic Ocean and Cape Town. The inset shows an outline of the peninsula with highlighting Cape Point (CPT) monitoring station and Cape Town City Center (CTCC).

Cape Point Gas Chromatograph-Mass Spectrometer

An Agilent gas chromatograph-mass spectrometer (GC-MS, 6890/5973N) with a custom-built adsorption/desorption system (ADS) was used to measure HCFC and HFC mole fractions in the atmosphere at Cape Point.[26] Air samples for analysis were drawn through a 15 m × ¼” OD (outside diameter) stainless steel sampling line from above the laboratory at ~17 l min^{-1} by a diaphragm pump (GAST, Miniature Diaphragm Pump 22D). Samples and standards were autonomously pre-concentrated on a triple bed microtrap (3 mg Carbotrap B; 5 mg Carboxen 1003 and 4 mg Carboxen 1000) at -50 ºC in the ADS.[27,28] Following pre-concentration on the microtrap, samples or standards were heated to 240 ºC and injected directly on to the column (CP Sil-5, 100m × 0.32 mm × 5 µm) at 240 ºC. Separation of the injected sample was achieved with a helium carrier flow (1.8 ml min^{-1}) and temperature programme with an initial isothermal period (30 ºC, 12 min) and temperature gradient (10 ºC min^{-1} to 150 ºC).

A short-term working standard, filled at Cape Point under baseline conditions, was analysed alternately to each air sample, to account for instrument drift. Calibrated mole fractions were assigned to short-term working standards from an external long-term working standard tank which was calibrated using the Advanced Global Atmospheric Gases Experiment (AGAGE) Medusa GC-MS at Mace Head.[29,30] The procedure provided a direct comparison of the short-term working standard with the relevant Scripps Institute of Oceanography (SIO) primary calibration scales.[29] The calibration of the long-term working standard (filled at Mace Head) had mole fraction values assigned from SIO-05 (HCFC-22 and HFC-152a) and SIO-14 (HFC-125). A complete description of the ADS-GC-MS system and set up can be found in Simmonds et al.[26]

Baseline classification algorithm

A statistical method based on the Advanced Global Atmospheric Gases Experiment (AGAGE) pollution algorithm was developed to identify baseline samples within long-lived trace gas mole fraction datasets. A full description can be found in the SI, the appendix to O'Doherty et al.[31] and Simmonds et al.[20] In brief, a second order polynomial is fitted to the daily minima over a rolling 121-day window, centered on each day of sampling with a period of 60 days either side of the sampling day. The polynomial was subtracted from each data point in the window, creating a matrix of distances. Measurements that were larger than 3 times the median of the distances were marked as 'polluted'. This was repeated until all of the data marked as 'polluted' were removed. Measurements between 2-3 times the median were marked as 'possibly polluted'. In the final step ‘possibly polluted’ measurements were tested for adjacency with ‘polluted’ measurements. Only the measurements of the sampling day were retained before the window moved to the subsequent day. The limited data towards the ends of the dataset may result in a small, but insignificant bias.

Atmospheric dispersion modeling using NAME

The U.K. Meteorological (Met.) Office’s Lagrangian atmospheric dispersion model, NAME (Numerical Atmospheric dispersion Modeling Environment), was used to simulate 30-day back-trajectories for each atmospheric measurement.[32] The NAME model was driven by meteorological fields derived from the operational analysis of the U.K. Met. Office Numerical Weather Prediction model, the Unified Model (UM), at an approximate horizontal resolution of 17 km in 2017 (reduced to ~12 km from 11th July 2017). The model domain spanned from 64° S to 4.3° N, and from 50° W to 87.3° E, covering southern Africa and the south Atlantic (Figure 2). Particles were released into the model domain from randomly generated points on a 20 m vertical line, centered on the Cape Point inlet (30 m above ground level) at a rate of 333 particles min^{-1}. All particles were assumed to be inert throughout the length of each 30-day simulation. Given the long lifetimes of the HCFC and HFCs studied here, this assumption can be made with very little loss of accuracy. At the edges of the NAME model domain, the 3-dimensional location and time at which each particle left the domain was recorded to provide sensitivity to mole fraction boundary conditions.

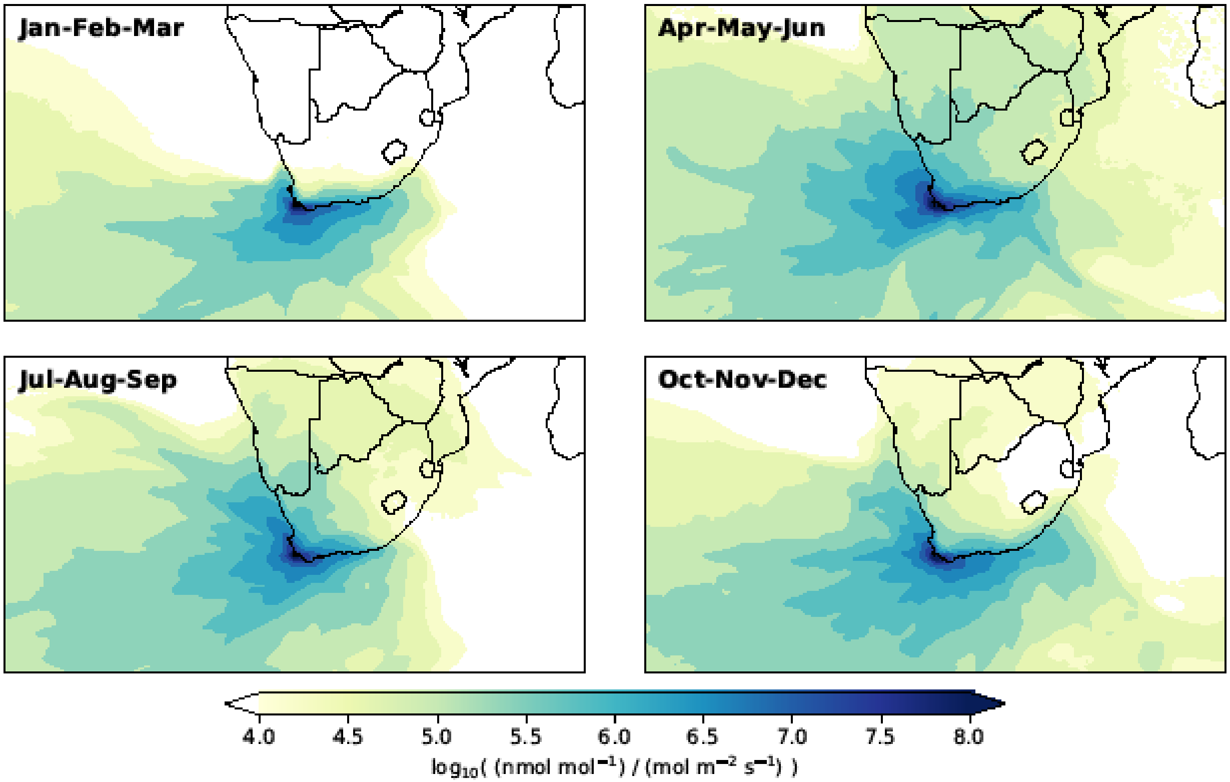

Figure 2. Mean 2017 quarterly air history footprints at Cape Point using the NAME model.

Estimating emissions using a hierarchical trans-dimensional Bayesian framework

A hierarchical trans-dimensional Bayesian framework was used to estimate South Africa's halocarbon emissions using the atmospheric measurements made at Cape Point. A full description of the inverse method can be found in Lunt et al.[33] The hierarchical treatment of uncertainties is described by Ganesan et al.[34] This inverse method has been used to estimate halocarbon emissions from other regions.[35,36] In short, the inverse approach attempts to solve for a parameters vector, $\boldsymbol{x}$ (including the flux grid and boundary conditions), using a set of atmospheric observations, $\boldsymbol{y}$. The system starts from an *a priori* flux field, $\boldsymbol{x_{ap}}$, which is adjusted using the atmospheric measurements in order to estimate the posterior flux field, $\boldsymbol{x}$, in conjunction with a linear model, **H**. **H** is a Jacobian matrix of sensitivities which describes the relationship between changes in atmospheric mole fraction and the parameters vector, $\boldsymbol{x}$. In a traditional Bayesian set-up, uncertainty in the *a priori* emissions ($\boldsymbol{x_{ap}}$) and model-measurement mismatch ($\boldsymbol{\varepsilon}$) are defined prior to the inversion. Hence, they are based on a subjective decision by the investigator. However, the choice of uncertainties has been shown to significantly influence the posterior solution. The hierarchical framework attempts to reduce the influence of this subjectivity by introducing hyper-parameters which define the uncertainties within these uncertainties.

A reversible-jump Markov Chain Monte Carlo algorithm (rj-MCMC) was used to estimate the posterior solution.[33] For each species, the rj-MCMC algorithm was run for a chain length of 400,000 iterations. The first 100,000 iterations were discarded to ensure that the system had no knowledge of the initial state. The remaining 300,000 iterations were then thinned via sub-sampling of every 100th iteration, resulting in 4000 samples, which were used to form the posterior PDFs. The emission estimates discussed in the following sections represent the means of these PDFs, with the corresponding uncertainty estimated to be the 95% confidence interval (2.5 – 97.5 percentile) of the same PDFs.

A priori emissions

Little detailed information is available for South Africa's halocarbon emissions. Therefore, *a priori* emissions were constructed from a variety of sources which together represent the existing state of knowledge. In the absence of emissions data, HCFC-22 a priori emissions were estimated using consumption data from South Africa's most recent HPMP report, which was estimated at 3.16 Gg yr^{-1} in 2009. In general, consumption is not a good approximation for emissions magnitudes (as, for this gas, emissions are likely dominated by release from the bank). However, as no estimates exist for South African emissions, we use consumption statistics as a proxy for emissions, but with a very large uncertainty (see below), on the assumption that they are of a similar order of magnitude to emissions. For HFC-125 and HFC-152a, emissions were taken from the EDGAR v4.2 emissions inventory, which reports gridded emissions data up to 2009. For all three gases, the a priori emissions total was distributed across the inverse model domain using the National Oceanic and Atmospheric Administration (NOAA) DMSP-OLS (Defence Meteorological Program - Operational Line-Scan System) satellite night-light data. These data are available at 30 arc second resolution (https://ngdc.noaa.gov/eog/data/web\textunderscore data/v4composites/). Night-lights have been shown to correlate with population density,[37] and hence this distribution is expected to be roughly representative of the sources of all three domestically consumed halocarbons. In each instance, the *a priori* emissions were given a 100% uncertainty, with the magnitude of this uncertainty further described by a uniform PDF with upper and lower bounds of 50% and 400% respectively. This PDF was explored within the inversion.

Boundary conditions

We incorporate boundary conditions to account for emissions from outside of the model domain. Uniform mole fraction 'curtains' were estimated using output from the AGAGE 12-box model; an extension of the work by Rigby et al.[38] The 12-box model resolves baseline mole fractions for four semi-hemispheres. For each month in which measurements were obtained, the simulated mole fraction from latitude bands 0-30° N, 0-30° S and 30-90° S were assigned to the North, East and West and South boundaries of the model domain respectively. The sensitivity of each measurement to the boundary conditions was estimated by mapping the exit locations of particles from the model domain for each measurement. The *a priori* boundary conditions were adjusted within the inversion.

RESULTS AND DISCUSSION

Cape Point measurements and observations

The baseline mole fractions of one hydrochlorofluorocarbon and two hydrofluorocarbons (HCFC-22, HFC-125, and HFC-152a) were determined from measurements made at the Cape Point Global Atmospheric Watch Station in 2017. The measurements were clustered along a baseline for the three species with occasional elevated data points (Figure 3). The mean mole fractions observed at Cape Point were: HCFC-22: 237.80 ± 12.31 ppt; HFC-125: 22.47 ± 1.78 ppt and HFC-152a: 6.44 ± 5.32 ppt. The Cape Point HCFC-22 and HFC-125 mole fractions increased throughout the year, in contrast with HFC-152a which displayed a small seasonal cycle. The increase through the year for HCFC-22 and HFC-125 was particularly noticeable for the last three months of 2017. Variability within the HCFC-22 and HFC-125 mole fractions, particularly in the early part of the year, were observed. Changes in wind direction, and therefore source contributions, likely contributed significantly to the observed variability.

The HFC-152a mole fraction increased between February and May, which continued in June. Following the winter maximum, the HFC-152a mole fractions decreased through the latter half of the year. The HFC-152a mole fractions increased at a lower rate at Cape Point, compared with HCFC-22 and HFC-125. The HFC-152a mole fractions displayed a maximum in austral winter and minima in February and October/November. The seasonal cycle observed in the HFC-152a mole fractions was likely driven by the austral winter minimum OH concentration. The shorter atmospheric lifetime of HFC-152a compared with HCFC-22 and HFC-125 highlights the sensitivity of this compound to reaction with OH, resulting in the observed seasonal cycle.

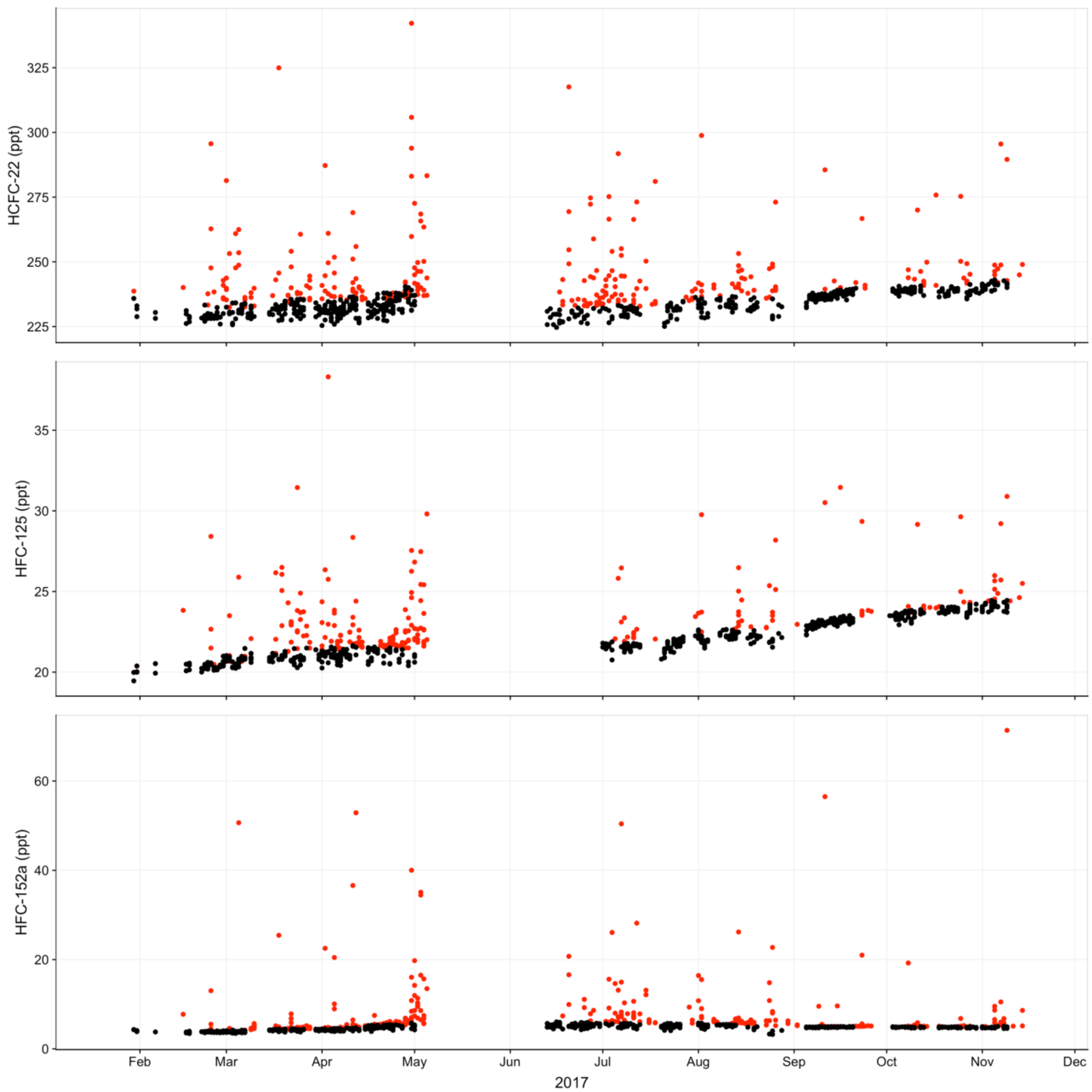

Figure 3. Time series of the HCFC and HFCs measured in the atmosphere at Cape Point. The gaps in the data represents instrument down time. Black points highlight the baseline measurements while red denote air from polluted sources.

The baselines within the Cape Point HCFC and HFC datasets were identified using the adapted AGAGE algorithm described in the Baseline Classification Algorithm in the Supplementary Information.[20,31] The algorithm relied on the iterative fitting of a second order quadratic function to the daily minima over a rolling 121-day window.[20,31] An analysis of the 'polluted' points identified by the pollution algorithm suggests that these were specific intrusions of anthropogenically modified air arriving at Cape Point. The mean baseline mole fractions from Cape Point were 233.50 ± 4.0 ppt, 21.95 ± 1.2 ppt, and 4.69 ± 0.5 ppt for HCFC-22, HFC-125 and HFC-152a, respectively. These mole fractions grew by 8.36 ppt yr^{-1}, 4.10 ppt yr^{-1} and 0.71 ppt yr^{-1} for HCFC-22, HFC-125 and HFC-152a, respectively, during the 2017 data acquisition window. The baseline growth rates and mean mole fractions reported here are in line with previous studies of the concentrations of these compounds in the atmosphere at another Southern Hemisphere site, Cape Grim (e.g. Simmonds et al.[14,20]).

The measurements made at Cape Point imply that the HCFC and HFCs share a common anthropogenic source situated in the wider City of Cape Town metropolitan area. A bivariate analysis of the HCFC and HFCs measurements from Cape Point indicate a good agreement with a dominant source to the north-east, most probably from stationary air conditioning units (Figure 4). HCFC-22 and HFC-125 appear to have a greater spread of sources, based on the air sampled at Cape Point, whereas HFC-152a seems to have a single dominant source located immediately to the north of Cape Point, as shown in the bivariate plots (Figure 4c). Interestingly, the pollution marked HCFC and HFCs measurements showed only marginal relationships ($r^2 < 0.5$) with known anthropogenic markers such as carbon monoxide and ^{222}Rn. The lack of relationship between HCFC and HFC mole fractions and anthropogenic markers observed here is consistent with previous studies of this kind (e.g. Rivett et al.[39,40], Mead et al.[41] and Khan et al.[42]). The

HCFC-22 and HFC-125 relationship displayed weak commonality in the pollution marked air, with an r^2 of 0.37.

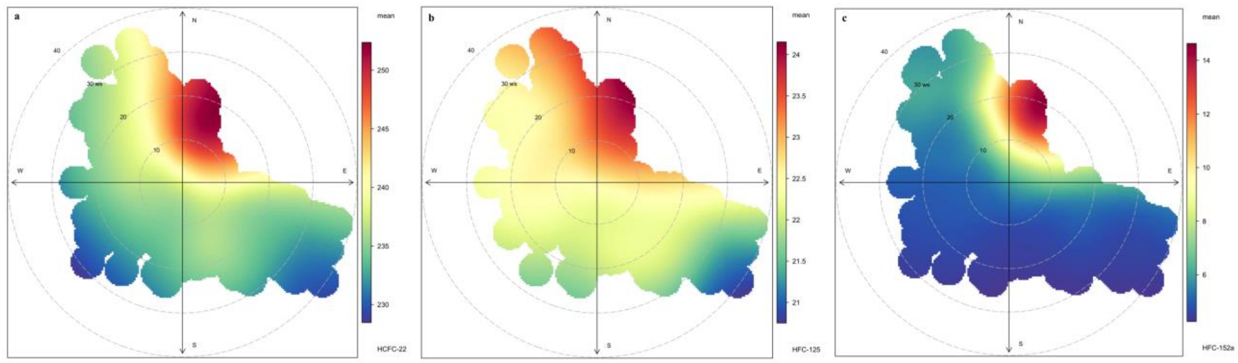

Figure 4. Bivariate plots for HCFC and HFC measurements at Cape Point. HCFC and HFC mole fractions displayed as a function of wind speed and direction for a. HCFC-22, b. HFC-125, and c. HFC-152a.

Estimation of South African HCFC-22, HFC-125 and HFC-152a emissions using an inverse model

When used in conjunction with an inverse model, long-term atmospheric measurements from the Cape Point observatory could potentially be used to estimate regional halocarbon emissions. In the absence of an annual bottom-up inventory, which South Africa is not currently required to submit, these top-down estimates could provide a useful means by which to track emissions from Africa's second largest economy. Given the considerable distance between Cape Point and populated areas such as Johannesburg, which are potentially significant sources of all three halocarbons discussed, estimating emissions for the entire country using the measurements presented here is not possible. We therefore derive emissions for a sub-domain named south western South Africa (SWSA), the extent of which is shown in Figure 5. The SWSA sub-domain is consistent with a region for which the average Cape Point NAME footprint (Figure 2) demonstrates appreciable sensitivity over the course of 2017.

Emissions from SWSA were estimated using the hierarchical trans-dimensional Bayesian framework described in the Methods section. The estimates presented in the following discussion are based on the mean value of each posterior probability density function (PDF), with an estimation of the corresponding uncertainty taken to be the 95% confidence interval of the same PDF. Posterior emissions and prior scaling maps are shown in Figure 5. A comparison of the atmospheric measurements with modeled mole fractions is shown in Figure S1. For each gas, the sensitivity of the inversion to changes in the magnitude of the prior is given in Figure S2.

The consumption (and emission) of all three gases are explicitly linked to population density through their use as refrigerants, foam blowing and aerosol applications. The SWSA sub-domain was estimated to account for 12.5% of South Africa's population.[43] Previous studies have shown that consumption (as opposed to production) is the predominant source of HCFC-22, HFC-125 and HFC-152a,[46,47] consequently population is expected to be a reasonable proxy for emissions. Hence, using the gridded population data,[43] the SWSA estimates were then extrapolated to estimate emissions for the whole of South Africa. While extrapolating in this manner is subject to its own uncertainties, we are unable to quantify these emissions estimates without additional measurements from elsewhere in South Africa.

We estimate SWSA HCFC-22 emissions to be 0.37 (0.20 – 0.55) Gg yr^{-1} in 2017. Our prior scaling map (Figure 5) suggests that the a priori emissions based on consumption statistics are an underestimate of emissions for most of the SWSA domain, consistent with the exclusion of emissions from refrigerant banks such as stationary air-conditioning units. Figure S2 suggests that the inversion is insensitive to changes in the magnitude of the prior. As expected, Cape Town is the dominant source of the enhanced HCFC-22 mole fractions observed at Cape Point, consistent with its use as a coolant for refrigeration and air-conditioning applications. We extrapolate SWSA emissions to a national total, estimating South Africa's HCFC-22 emissions to be 3.0 (1.6 – 4.4) Gg yr^{-1} in 2017. Simmonds et al.[14] estimated global HCFC-22 emissions of 370.3 ± 45.9 Gg yr^{-1} in 2016. When placed in context to the global burden, South Africa's HCFC-22 emissions (0.8% of the global total) are relatively small. Saikawa et al.[44] estimated combined African and Middle Eastern HCFC-22 emissions of 36.4 ± 22.3 Gg yr^{-1} for 2009. Assuming that this total did not change significantly between 2009 and 2017, South Africa could account for ~8% of HCFC-22 emissions from this region. Nevertheless, emissions from the African continent as a whole are comparatively small. As a comparison, Asian Annex 5 countries emitted 213 ± 20.8 Gg yr^{-1} in the same year.[44]

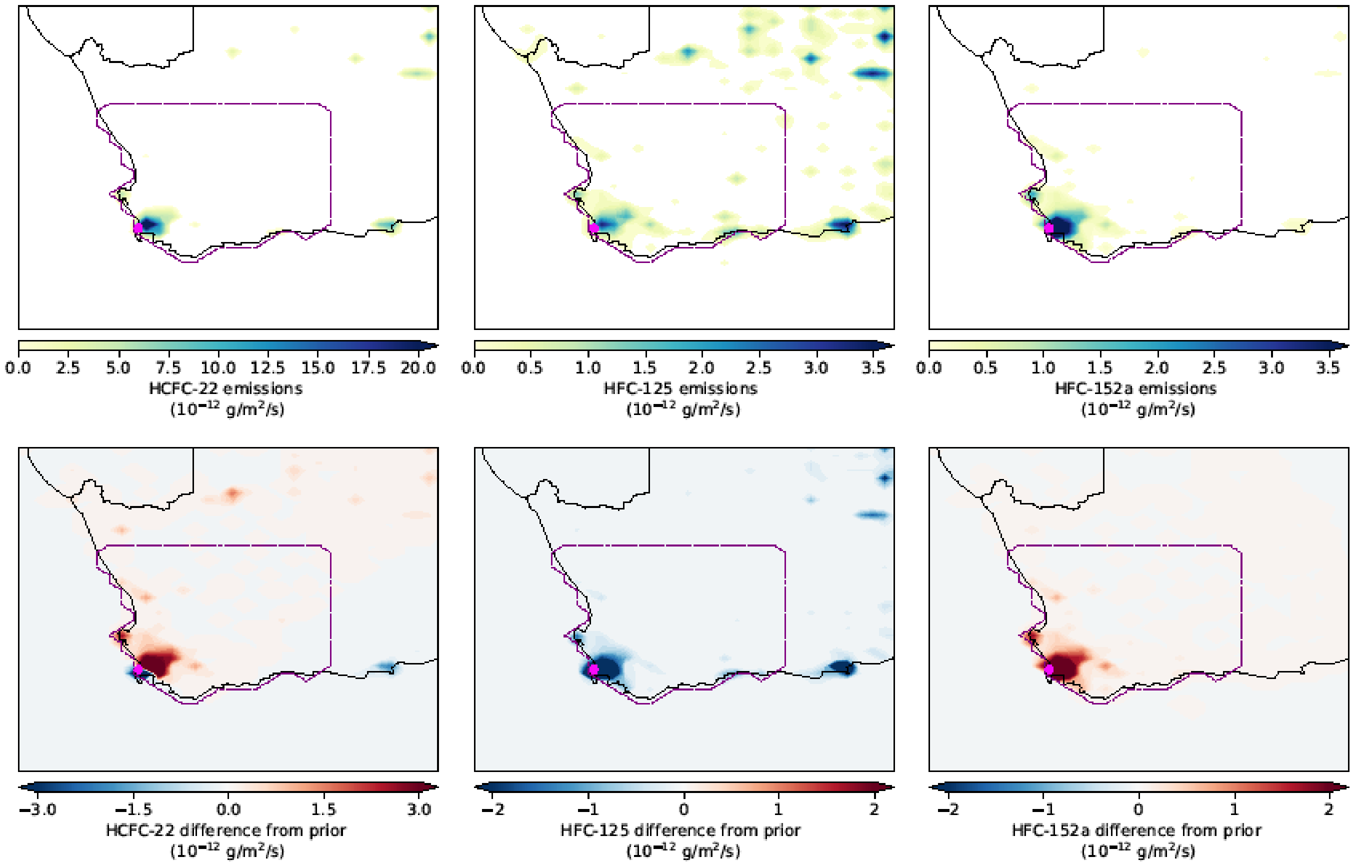

Figure 5. Top) Maps of the posterior distribution of emissions of HCFC-22, HFC-125 and HFC-152a, based on measurements from the Cape Point monitoring station. Bottom) Maps of the difference between posterior and prior distributions of emissions, presented in the same units as above. Red indicates regions where the posterior was larger than the prior emissions field. The purple dashed line indicates the boundaries of the south western South Africa (SWSA) model sub-domain, and the pink circle indicates the location of Cape Town.

With consumption of HCFCs now regulated under the Montreal Protocol, it is widely expected that South Africa will accelerate its adoption of non-ozone depleting alternatives. R-410A (a zeotropic 50:50 blend of HFC-125 and HFC-32) is commonly cited as a replacement for HCFC-22 in refrigeration systems.[50] We estimate SWSA HFC-125 emissions of 0.1 (0.06 – 0.15) Gg yr-

^{1} in 2017. As with HCFC-22, the dominant source was found to be Cape Town (Figure 5). Extrapolating to a national total, we estimate South Africa's HFC-125 emissions to be 0.8 (0.5 – 1.2) Gg yr^{-1}. Assuming HFC-125 blends to be the most common replacement for HCFC-22, our results suggest that South Africa's stationary refrigerant demands are still met predominantly by HCFC-22, as opposed to the non-ozone depleting alternatives. Simmonds et al.[12] estimated global HFC-125 emissions of 59.7 ± 9.5 Gg yr^{-1} for 2015, hence South Africa represents approximately 1.3% of the global total.

As with HFC-125, South Africa's emissions of HFC-152a might be expected to increase as it replaces ozone-depleting alternatives (e.g. HCFC-141b and HCFC-142b) in applications such as foam-blowing and as an aerosol propellant. HFC-152a has also been proposed as a replacement for HFC-134a in mobile air-conditioning units, due to its significantly lower GWP_{100}. We estimate SWSA HFC-152a emissions to be 0.14 (0.08 – 0.20) Gg yr^{-1} in 2017. Our prior scaling map suggests that the prior is a significant underestimation of emissions across much of the SWSA model domain, consistent with significant growth in emissions since 2009 (the last year reported by EDGAR), or discrepancies between top-down and bottom-up reporting methods. We extrapolate our SWSA emissions to a national total, estimating South Africa's HFC-152a emissions to be 1.1 (0.64 – 1.6) Gg yr^{-1}. Simmonds et al.[20] estimated global HFC-152a emissions to be 52.5 ± 20.1 Gg yr^{-1} in 2014. Assuming this total to have not changed significantly in the proceeding 3 years, South Africa could account for ~2.1 % of global emissions in 2017.

As an Article-5 country, South Africa is not currently required to publish a detailed inventory of its greenhouse gas emissions.[15] Except for consumption statistics submitted as part of its Montreal Protocol commitments, which do not consider emissions from banks, South Africa's HCFC and HFC emissions are poorly defined. In accordance with the HPMP, South Africa was required to freeze its HCFC consumption by 2013 (relative to a 2009/10 baseline) followed by successive cuts leading to a complete phase-out by 2030. South Africa is also in the process of ratifying the Kigali Amendment to the Montreal Protocol, which sets out plans to reduce global emissions of HFCs and came into effect on January 1st, 2019. However, South Africa will not be required to freeze its production or consumption of HFCs until 2024. Given the current and impending regulations imposed on South Africa's halocarbon emissions, in the absence of a nationwide monitoring programme for these compounds, plausible estimates of the country's emissions are useful. Ongoing atmospheric measurements of key HCFC and HFC mole fractions at Cape Point provide a valuable means by which to verify South Africa's progress under the Kigali Amendment.

Further work is required to verify the results of this study, if these estimates are to form a reliable means of validation for future inventory work. The usefulness of Cape Point as a means by which to estimate South Africa's halocarbon emissions is also likely to increase as the dataset grows. In particular, more data collected during the Southern Hemisphere autumn and winter months - which corresponds with a maximum in the sensitivity of the site to terrestrial sources – would be highly beneficial. In addition, further measurements from the east of the country, with improved sensitivity to major population centers such as Johannesburg, would provide further constraint on South Africa's halocarbon emissions.

ASSOCIATED CONTENT

Supporting Information

The Supporting Information is available free of charge on the ACS Publications website.

Baseline classification algorithm; comparison of measured and modeled mole fractions of HCFC and HFCs at Cape Point (Figure S1); sensitivity plots showing the change in SWSA posterior emissions as a result of scaling (50% - 200%) of the prior (Figure S2)

Measurement data and model code availability

The measurement data and baseline code can be obtained upon request from Brett Kuyper (brett.kuyper@gmail.com) and the inverse model code used in this study is available upon request from Matt Rigby (Matt.Rigby@bristol.ac.uk). The NAME model is available upon request from the UK Met Office.

AUTHOR INFORMATION

Corresponding author

*E-mail: d.e.shallcross@bristol.ac.uk, Tel: +44 117 928 7796

NOTES

The authors declare no competing financial interest.

ACKNOWLEDGEMENTS

We thank a variety of funders under whose auspices this work was carried out including Bristol ChemLabS Outreach, Primary Science Teaching Trust (MAHK) and NERC grants NE/M014851/1 and NE/I027282/1 (DS). The authors would like to thank the Universities of Bristol and the Western Cape for their support. The authors would like to thank Gerry Spain at Mace Head for his help with filing the long-term standard tank and the analysing of it. The authors would like to thank William J Whittaker for his assistance in decoding the AGAGE pollution algorithm.

REFERENCES

(1) Derwent, R. G.; Volz-Thomas, A. The Tropospheric Lifetimes of Halocarbons and Their Reactions with OH Radicals: An Assessment Based on the Concentration of ^{14}CO. In *UNEP/WMO Scientific Assessment of Stratospheric Ozone*; 1989; p Appendix.

(2) Liu, R.; Huie, R. E.; Kurylo, M. J. Rate Constants for the Reactions of the OH Radical

with Some Hydrochlorofluorocarbons over the Temperature Range 270-400 K. *J.Phys.Chem.* **1990**, *94* (7), 3247–3249; https://doi.org/10.1021/j100371a004.

(3) Fisher, D. A.; Hales, C. H.; Filkin, D. L.; Ko, M. K. W.; Sze, N. D.; Connell, P. S.; Wuebbles, D. J.; Isaksen, I. S. A.; Stordal, F. Model Calculations of the Relative Effects of CFCs and Their Replacements on Stratospheric Ozone. *Nature* **1990**, *344* (6266), 508–512; https://doi.org/10.1038/344508a0.

(4) Naik, V.; Jain, A. K.; Patten, K. O.; Wuebbles, D. J. Consistent Sets of Atmospheric Lifetimes and Radiative Forcings on Climate for CFC Replacements: HCFCs and HFCs. *J. Geophys. Res. Atmos.* **2000**, *105* (D5), 6903–6914; https://doi.org/10.1029/1999JD901128.

(5) Velders, G. J. M. M.; Fahey, D. W.; Daniel, J. S.; McFarland, M.; Andersen, S. O. The Large Contribution of Projected HFC Emissions to Future Climate Forcing. *Proc. Natl. Acad. Sci. U. S. A.* **2009**, *106* (27), 10949–10954; https://doi.org/10.1073/pnas.0902817106.

(6) Papanastasiou, D. K.; Beltrone, A.; Marshall, P.; Burkholder, J. B. Global Warming Potential Estimates for the C_1 – C_3 Hydrochlorofluorocarbons (HCFCs) Included in the Kigali Amendment to the Montreal Protocol. *Atmos. Chem. Phys.* **2018**, *18*, 6317–6330; https://doi.org/10.5194/acp-18-6317-2018

(7) UNEP - Ozone Secretariat. *Amendement to the Montreal Protocol on Substances That Deplete the Ozone Layer: Report*; Copenhagen, 1992.

(8) UNEP - Ozone Secretariat. *Amendment to the Montreal Protocol on Substances That*

Deplete the Ozone Layer: Report; Kigali, 2016.

(9) NEDLAC. *Hydrochlorofluorocarbons (HCFC) Phase Out Plan for South Africa*; National Economic Development and Labour Council, Department of Environmental Affairs: Johannesburg, 2012.

(10) WMO. *Scientific Assessment of Ozone Depletion: 2014*; World Meteorological Organization, 2014.

(11) Rinsland, C. P.; Chiou, L.; Boone, C.; Bernath, P.; Mahieu, E. First Measurements of the HCFC-142b Trend from Atmospheric Chemistry Experiment (ACE) Solar Occultation Spectra. *J. Quant. Spectrosc. Radiat. Transf.* **2009**, *110* (18), 2127–2134; https://doi.org/10.1016/j.jqsrt.2009.05.011.

(12) Simmonds, P. G.; Rigby, M.; McCulloch, A.; O'Doherty, S. J.; Young, D.; Mühle, J.; Krummel, P. B.; Steele, L. P.; Fraser, P. J.; Manning, A. J.; et al. Changing Trends and Emissions of Hydrochlorofluorocarbons (HCFCs) and Their Hydrofluorocarbon (HFCs) Replacements. *Atmos. Chem. Phys.* **2017**, *17* (7), 4641–4655; https://doi.org/10.5194/acp-17-4641-2017.

(13) Burkholder, J. B.; Cox, R. A.; Ravishankara, A. R. Atmospheric Degradation of Ozone Depleting Substances, Their Substitutes, and Related Species. *Chem. Rev.* **2015**, *115* (10), 3704–3759; https://doi.org/10.1021/cr5006759.

(14) Simmonds, P. G.; Rigby, M.; McCulloch, A.; Vollmer, M. K.; Henne, S.; Mühle, J.; O'Doherty, S. J.; Manning, A. J.; Krummel, P. B.; Fraser, P. J.; et al. Recent Increases in the Atmospheric Growth Rate and Emissions of HFC-23 (CHF_3) and the Link to HCFC-

22 ($CHClF_2$) Production. *Atmos. Chem. Phys.* **2018**, *18* (6), 4153–4169; https://doi.org/10.5194/acp-18-4153-2018.

(15) Graziosi, F.; Arduini, J.; Furlani, F.; Giostra, U.; Kuijpers, L. J. M.; Montzka, S. A.; Miller, B. R.; O'Doherty, S. J.; Stohl, A.; Bonasoni, P.; et al. European Emissions of HCFC-22 Based on Eleven Years of High Frequency Atmospheric Measurements and a Bayesian Inversion Method. *Atmos. Environ.* **2015**, *112*, 196–207; https://doi.org/10.1016/j.atmosenv.2015.04.042.

(16) Aucott, M. L.; McCulloch, A.; Graedel, T. E.; Kleiman, G.; Midgley, P.; Li, Y.-F. Anthropogenic Emissions of Trichloromethane (Chloroform CHCl<sub>3\<sub>) and Chlorodifluoromethane (HCFC-22): Reactive Chlorine Emissions Inventory. *J. Geophys. Res.* **1999**, *104* (D7), 8405–8415; https://doi.org/10.1029/1999JD900053.

(17) Xiang, B.; Patra, P. K.; Montzka, S. A.; Miller, S. M.; Elkins, J. W.; Moore, F. L.; Atlas, E. L.; Miller, B. R.; Weiss, R. F.; Prinn, R. G.; et al. Global Emissions of Refrigerants HCFC-22 and HFC-134a: Unforeseen Seasonal Contributions. *Proc. Natl. Acad. Sci.* **2014**, *111* (49), 17379–17384; https://doi.org/10.1073/pnas.1417372111.

(18) Forster, P.; Ramaswamy, V.; Artaxo, P.; Berntsen, T.; Betts, R.; Fahey, D. W.; Haywood, J.; Lean, J.; Lowe, D. C.; Myhre, G.; et al. Climate Change 2007: The Physical Science Basis. Contribution of Working Group I to the Fourth Assessment Report of the Intergovernmental Panel on Climate Change. Chapter 2: Changes in Atmospheric and Radiative Forcing. *Cambridge Univ. Press* **2007**, 129–234; https://doi.org/10.1103/PhysRevB.77.220407.

(19) O'Doherty, S. J.; Miller, B. R.; Mühle, J.; McCulloch, A.; Simmonds, R. G.; Manning, A.

J.; Reimann, S.; Vollmer, M. K.; Greally, B. R.; Prinn, R. G.; et al. Global and Regional Emissions of HFC-125 (CHF2CF3) from in Situ and Air Archive Atmospheric Observations at AGAGE and SOGE Observatories. *J. Geophys. Res. Atmos.* **2009**, *114* (23); https://doi.org/10.1029/2009JD012184.

(20) Simmonds, P. G.; Rigby, M.; Manning, A. J.; Lunt, M. F.; O'Doherty, S. J.; McCulloch, A.; Fraser, P. J.; Henne, S.; Vollmer, M. K.; Mühle, J.; et al. Global and Regional Emissions Estimates of 1,1-Difluoroethane (HFC-152a, CH_3CHF_2) from in Situ and Air Archive Observations. *Atmos. Chem. Phys.* **2016**, *16* (1), 365–382; https://doi.org/10.5194/acp-16-365-2016.

(21) Labuschagne, C.; Kuyper, B.; Brunke, E.; Spuy, D. Van Der; Martin, L.; Mbambalala, E.; Khan, M. A. H.; Davies-coleman, M. T.; Shallcross, D. E.; Joubert, W. A Review of Four Decades of Atmospheric Trace Gas Measurements at Cape Point, South Africa. *Trans. R. Soc. South Africa* **2018**, 1–20; https://doi.org/10.1080/0035919X.2018.1477854.

(22) Tyson, P. D.; Preston-Whyte, R. A. *The Weather and Climate of Southern Africa*; Oxford University Press Southern Africa: Cape Town, 2000.

(23) Preston-Whyte, R. A.; Tyson, P. D. *The Atmosphere and Weather of Southern Africa*; Oxford University Press: Oxford, U.K., 1993.

(24) Garstang, M.; Tyson, P. D.; Edwards, M.; Kallberg, P.; Lindesay, J. A. Horizontal and Vertical Transport of Air over Southern Africa. *J. Geophys. Res.* **1996**, *101* (D19), 23721–23736; https://doi.org/10.1029/95JD00844.

(25) Brunke, E.; Walters, C.; Mkololo, T.; Martin, L. G.; Labuschagne, C.; Silwana, B.; Slemr,

F.; Weigelt, A.; Ebinghaus, R.; Somerset, V. Mercury in the Atmosphere and in Rainwater at Cape Point, South Africa. *Atmos. Environ.* **2016**, *125*, 24–32; https://doi.org/10.1016/j.atmosenv.2015.10.059.

(26) Simmonds, P. G.; O'Doherty, S. J.; Nickless, G.; Sturrock, G. A.; Swaby, R.; Knight, P.; Ricketts, J.; Woffendin, G.; Smith, R. Automated Gas Chromatograph/Mass Spectrometer for Routine Atmospheric Field Measurements of the CFC Replacement Compounds, the Hydrofluorocarbons and Hydrochlorofluorocarbons. *Anal. Chem.* **1995**, *67* (4), 717–723; https://doi.org/10.1021/ac00100a005.

(27) O'Doherty, S. J.; Simmonds, P. G.; Nickless, G.; Betz, W. R. Evaluation of Carboxen Carbon Molecular Sieves for Trapping Replacement Chlorofluorocarbons. *J. Chromatogr.* **1993**, *630*, 265–274; https://doi.org/10.2989/02577619209504717.

(28) Sturrock, G. A.; Porter, L. W.; Fraser, P. J. In Situ Measurement of CFC Replacement Chemicals and Other Halocarbons at Cape Grim: The AGAGE GC-MS Program. In *Baseline 97–98*; Tindale, N. W., Derek, N., Francey, R. J., Eds.; Bureau of Meteorology, CSIRO: Melbourne, Victoria, 2001; pp 43–49.

(29) Miller, B. R.; Weiss, R. F.; Salameh, P. K.; Tanhua, T.; Greally, B. R.; Mühle, J.; Simmonds, P. G. Medusa: A Sample Preconcentration and GC-MS Detector System for in Situ Measurements of Atmospheric Trace Halocarbons, Hydrocarbons and Sulfur Compounds. *Anal. Chem.* **2008**, *80* (1), 1536–1545; https://doi.org/10.1021/ac702084k.

(30) Arnold, T.; Mühle, J.; Salameh, P. K.; Harth, C. M.; Ivy, D. J.; Weiss, R. F. Automated Measurement of Nitrogen Trifluoride in Ambient Air. *Anal. Chem.* **2012**, *84*, 4798–4804; https://doi.org/10.1021/ac300373e.

(31) O'Doherty, S. J.; Simmonds, P. G.; Cunnold, D. M.; Wang, H. J.; Sturrock, G. A.; Fraser, P. J.; Ryall, D. B.; Derwent, R. G.; Weiss, R. F.; Salameh, P. K.; et al. In Situ Chloroform Measurements at Advanced Global Atmospheric Gases Experiment Atmospheric Research Stations from 1994 to 1998. *J. Geophys. Res. Atmos.* **2001**, *106* (D17), 20429–20444; https://doi.org/10.1029/2000JD900792.

(32) Manning, A. J.; O'Doherty, S. J.; Jones, A. R.; Simmonds, P. G.; Derwent, R. G. Estimating UK Methane and Nitrous Oxide Emissions from 1990 to 2007 Using an Inversion Modeling Approach. *J. Geophys. Res. Atmos.* **2011**, *116* (2), 1–19; https://doi.org/10.1029/2010JD014763.

(33) Lunt, M. F.; Rigby, M.; Ganesan, A. L.; Manning, A. J. Estimation of Trace Gas Fluxes with Objectively Determined Basis Functions Using Reversible-Jump Markov Chain Monte Carlo. *Geosci. Model Dev.* **2016**, *9* (9), 3213–3229; https://doi.org/10.5194/gmd-9-3213-2016.

(34) Ganesan, A. L.; Rigby, M.; Zammit-Mangion, A.; Manning, A. J.; Prinn, R. G.; Fraser, P. J.; Harth, C. M.; Kim, K. R.; Krummel, P. B.; Li, S.; et al. Characterization of Uncertainties in Atmospheric Trace Gas Inversions Using Hierarchical Bayesian Methods. *Atmos. Chem. Phys.* **2014**, *14* (8), 3855–3864; https://doi.org/10.5194/acp-14-3855-2014.

(35) Lunt, M. F.; Park, S.; Li, S.; Henne, S.; Manning, A. J.; Ganesan, A. L.; Simpson, I. J.; Blake, D. R.; Liang, Q.; O'Doherty, S.; et al. Continued Emissions of the Ozone-Depleting Substance Carbon Tetrachloride From Eastern Asia. *Geophys. Res. Lett.* **2018**, *4*, 423–430; https://doi.org/10.1029/2018GL079500.

(36) Say, D.; Ganesan, A. L.; Lunt, M. F.; Rigby, M.; O'Doherty, S.; Harth, C.; Manning, A.

J.; Krummel, P. B.; Bauguitte, S. Atmospheric observations and emission estimates of ozone-depleting chlorocarbons from India. *Atmos. Chem. Phys. Discuss.* **2018**; https://doi.org/10.5194/acp-2018-1287.

(37) Raupach, M. R.; Rayner, P. J.; Paget, M. Regional Variations in Spatial Structure of Nightlights, Population Density and Fossil-Fuel CO2emissions. *Energy Policy* **2010**, *38* (9), 4756–4764; https://doi.org/10.1016/j.enpol.2009.08.021.

(38) Rigby, M.; Prinn, R. G.; O'Doherty, S. J.; Miller, B. R.; Ivy, D.; Mühle, J.; Harth, C. M.; Salameh, P. K.; Arnold, T.; Weiss, R. F.; et al. Recent and Future Trends in Synthetic Greenhouse Gas Radiative Forcing. *Geophys. Res. Lett.* **2014**, *41* (7), 2623–2630; https://doi.org/10.1002/2013GL059099.

(39) Rivett, A. C.; Martin, D.; Nickless, G.; Simmonds, P. G.; O'Doherty, S. J.; Gray, D. J.; Shallcross, D. E. In Situ Gas Chromatographic Measurements of Halocarbons in an Urban Environment. *Atmos. Environ.* **2003**, *37* (16), 2221–2235; https://doi.org/10.1016/S1352-2310(03)00148-1.

(40) Rivett, A. C.; Martin, D.; Gray, D. J.; Price, C. S.; Nickless, G.; Simmonds, P. G.; O'Doherty, S. J.; Greally, B. R.; Knights, A.; Shallcross, D. E. The Role of Volatile Organic Compounds in the Polluted Urban Atmosphere of Bristol, England. *Atmos. Chem. Phys.* **2003**, *3* (4), 1165–1176; https://doi.org/10.5194/acp-3-1165-2003.

(41) Mead, M. I.; Khan, M. A. H.; Bull, I. D.; White, I. R.; Nickless, G.; Shallcross, D. E. Stable Carbon Isotope Analysis of Selected Halocarbons at Parts per Trillion Concentration in an Urban Location. *Environ. Chem.* **2008**, *5* (5), 340–346; https://doi.org/10.1071/EN08037.

(42) Khan, M. A. H.; Mead, M. I.; White, I. R.; Golledge, B.; Nickless, G.; Knights, A.; Martin, D.; Rivett, A. C.; Greally, B. R.; Shallcross, D. E. Year-Long Measurements of C_1-C_3 Halocarbons at an Urban Site and Their Relationship with Meteorological Parameters. *Atmos. Sci. Lett.* **2009**, *10*, 75–86; https://doi.org/10.1002/asl.

(43) Center for International Earth Science Information Network (CIESIN). *Documentation for Gridded Population of the World, Version 4 (GPWv4)*; NASA Socioeconomic Data and Applications Center (SEDAC): Palisades, NY, 2016; https://doi.org/http://dx.doi.org/10.7927/H4D50JX4.

(44) Saikawa, E.; Rigby, M.; Prinn, R. G.; Montzka, S. A.; Miller, B. R.; Kuijpers, L. J. M.; Fraser, P. J. B.; Vollmer, M. K.; Saito, T.; Yokouchi, Y.; et al. Global and Regional Emission Estimates for HCFC-22. *Atmos. Chem. Phys.* **2012**, *12* (21), 10033–10050; https://doi.org/10.5194/acp-12-10033-2012.